Comparison of Two- and Three-Dimensional Model Simulation of the Effect of a Tidal Barrier on the Gulf of Maine Tides

PETER V. SUCSY, BRYAN R. PEARCE, AND VIJAY G. PANCHANG

Department of Civil Engineering, University of Maine, Orono, Maine

(Manuscript received 8 February 1991, in final form 29 September 1992)

ABSTRACT

Two-dimensional and three-dimensional tide models were used to simulate the M_2 tide in the Gulf of Maine. Model estimates of changes to the tide caused by a tidal barrier in the upper Bay of Fundy were made and compared. Tidal amplitudes in the presence of a barrier increased 30–50 cm for both models, corroborating the results of previous studies by Greenberg and by Duff. The three-dimensional model uniformly produced postbarrier elevations of 3.5 cm less than the two-dimensional model in the Gulf of Maine.

A comparison of model amplitudes and velocities with data for the existing M_2 tide is provided for both models. Total frictional dissipation is also calculated for each model and compared. Finally, the postbarrier amplitudes as predicted by each model are compared.

Root-mean-square errors of M_2 tidal amplitude and phase at 45 locations in the Gulf of Maine were 7.9 cm and 6° for the two-dimensional model and 5.7 cm and 7° for the three-dimensional model. Both models predicted essentially identical frictional dissipations for the Gulf of Maine of 4.8–4.9 $\times$ 10^{10} watts. Spatial differences in dissipation did not alter model predictions of well-mixed regions in the gulf based on a vertical mixing parameter used by Garrett et al. for the same region.

1. Introduction

The Gulf of Maine (Fig. 1) is a coastal sea approximately 400 km long and 200 km wide and forms the U.S. coastline from Cape Cod to New Brunswick. The Bay of Fundy is an extension of the northeast corner of the Gulf, and together the Gulf of Maine and Bay of Fundy form a tidal system in resonance with the M_2 amplitudes at the head of the Bay of Fundy of over 5 m.

The Canadian government, and in particular the Tidal Power Corporation of Halifax, Nova Scotia, have plans to build a tidal power dam in the upper reaches of the Bay of Fundy. The enormous tides of that region could provide a substantial amount of electrical power to eastern Canada as well as to the New England states. Previous modeling studies (Garrett 1974; Greenberg 1977, 1979; Duff 1981), however, have indicated that the construction of a barrier in the Bay of Fundy would increase the tidal amplitudes in the Gulf of Maine as far away as Boston on the opposite side of the gulf. Of these studies, the Greenberg study is regarded as the most accurate assessment of the effects of barriers on the tides. He reported a 20-cm increase in the tidal amplitude at Boston for a barrier placed across Minas Channel. It is presently the position of the Tidal Power Corporation that the possibility of increased tides on the New England coast remains a "potential project-stopper."

Previous modeling studies of the effects of barriers on the tides in the Gulf of Maine have used two-dimensional vertically averaged models. Garrett (1974) used the "resonance iteration" numerical method of Platzman, which neglects friction, with a grid size of approximately 25 km to determine the normal mode frequencies of the gulf and estimate changes to the tides by tidal dam construction. He concluded that a barrier placed in the Bay of Fundy would raise the M_2 tide in the Gulf of Maine because the new system would be in closer resonance with the tide, and because of a change of shape of the normal mode. Garrett estimated an increase of 25% in the M_2 amplitude at Boston for an impermeable barrier placed across Minas Basin. Greenberg (1977, 1979) used a conventional two-dimensional tide model with a nested finite-difference grid of 21-, 7-, and 2.3-km grid scale to simulate the existing and postbarrier tides. The Greenberg model incorporated friction by use of a quadratic bottom stress law based on vertically averaged velocities. Greenberg's results corroborated the Garrett study and provided

Corresponding author address: Dr. Peter V. Sucsy, Department of Civil Engineering, University of Maine, 456 Aubert Hall, Orono, ME 04469.

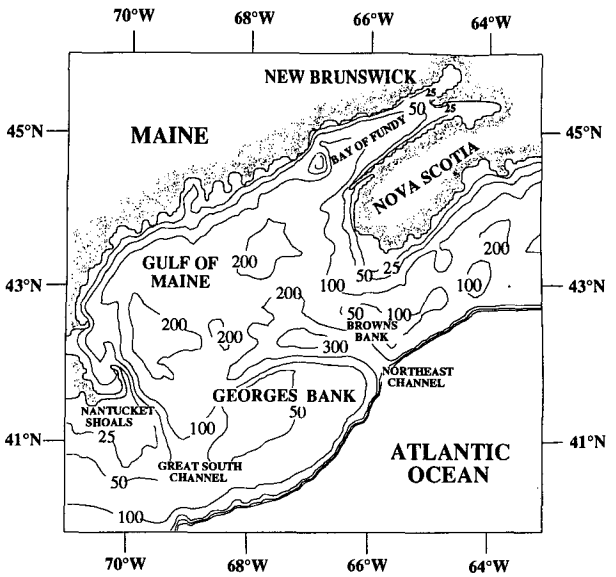

FIG. 1. Features of Gulf of Maine bathymetry constructed from model grid of approximately 5-km resolution.

greater spatial resolution. Greenberg estimated that an impermeable barrier placed across Minas Basin would increase the M_2 tide at Boston by 33%. Duff (1981) used a two-dimensional global tide model that incorporated the entire North Atlantic into the model area in order to examine the relative effects of the open boundary on the model solutions. Duff's model also incorporated friction using a vertically averaged quadratic bottom stress law. Duff's study contains important results related to the open boundary problem, but the model resolution was too coarse in the western Gulf of Maine and over Georges Bank to make reliable estimates of the effect of a tidal barrier on the tide in those regions.

To date, a three-dimensional tide model has not been used to investigate the effect of a tidal barrage on the Gulf of Maine tides. The primary goal of this research was to determine whether differences in the specification of bottom friction between two-dimensional and three-dimensional tide models would affect model results. Bottom friction for the two-dimensional model is parameterized as a function of the vertically averaged velocity, while for the three-dimensional model bottom stress is a function of the velocity at the top of the bottom boundary layer. In the Gulf of Maine, the near-bottom M_2 tidal velocity differs from the vertically averaged velocity in both magnitude and direction (Brown 1984). The three-dimensional bottom stress parameterization should thus provide a more realistic estimate of the phase and direction of the actual bottom stress.

Davies and Furnes (1980) found that the specification of bottom friction in terms of the vertically averaged velocity rather than the velocity at the top of the boundary layer introduced significant errors in a tide model solution for the North Sea. Davies compared the results of a three-dimensional tide model of the North Sea with a two-dimensional tide model by Flather (1976). The tidal amplitudes and vertically averaged velocities calculated by the two models were comparable. The distribution of errors was markedly different, however. The two-dimensional model consistently overestimated the phase error, while the three-dimensional model errors were symmetrically distributed. Davies concludes that the bias for error distribution in the two-dimensional model is due to the poor representation of the bottom stress. A tide modeling study of Puget Sound by Chu et al. (1989), however, showed no significant difference between elevations or phases calculated by a three-dimensional and two-dimensional model. The three-dimensional model used for this study was a layered model that used only two layers in the vertical and may have lacked sufficient vertical resolution.

The question to be addressed in the present study is the behavior of a three-dimensional model after the inclusion of a tidal barrier in the Bay of Fundy. Brown (1984) pointed out that the near-resonant physics of the Gulf of Maine is probably sensitive to dissipation rates. The different formulation of bottom friction in a three-dimensional model could thus produce spatially different dissipation rates and correspondingly different predictions of tidal amplitudes in the presence of a tide barrier. A three-dimensional tide model was thus used to determine both the spatial variability in dissipation rates between the two- and three-dimensional model and each model's comparative prediction of M_2 tidal elevations in the presence of a barrier.

A secondary goal of this study was to provide an independent tide model to corroborate the Greenberg study. Justification for providing an additional, independent model study was based on the sensitivity of numerical tide models of this region to grid resolution, geometry, and bathymetry. In fact, Gulf of Maine tide models are extremely sensitive to bathymetry, because of the unique proximity of the free period of the Gulf to the forced M_2 tidal period (Sucsy et al. 1990). A similar sensitivity was found for small errors in grid size of the same order as the distortion in dimensions from Mercator projected charts of the gulf (Sucsy 1990). Grid resolution affects the models ability to reproduce sharp horizontal gradients in amplitude and phase and also affects the quality of model bathymetry and geometry.

We thus implemented both a standard two-dimensional, vertically averaged tide model similar to the Greenberg model (Greenberg 1977, 1983) and a three-dimensional spectral tide model. The models were then applied to an independently constructed grid of the region. This was a uniform finite-difference grid with approximately 5.0 km $\times$ 5.5 km cells over the entire region. Greenberg used a nested finite-difference grid

with cell dimensions of 21 km in the Gulf of Maine that was reduced to 7 km in the outer Bay of Fundy and near 2.3 km in the upper Bay of Fundy. The bathymetric dataset was independently constructed from navigational charts and the models tuned by adjusting the bottom friction factors and coefficient of horizontal and vertical eddy viscosity (for the three-dimensional model) to match the existing M_2 tide at 45 locations of known data. The target accuracy was 10% error for amplitudes and 20° for phase. Each model was then run with an impermeable barrier placed across Minas Basin, a scenario identical to one that resulted in the largest alteration to the tide at Boston in the 1977 Greenberg study. The results confirmed Greenberg's original study, that a tidal barrier placed in the Bay of Fundy would increase the tidal amplitudes along the U.S. East Coast.

The three-dimensional model did not differ from the two-dimensional model in ability to replicate the existing tide. The rms error for existing M_2 amplitude and phase at 45 stations throughout the Gulf of Maine was 7.9 cm and 6 deg for the two-dimensional model, and 5.7 cm and 7 deg for the three-dimensional model. Computed M_2 tidal amplitudes were slightly less affected by the addition of a tidal barrier for the three-dimensional compared to the two-dimensional model for elevations along the coast of Maine. In general, the three-dimensional model elevations along the Maine coast, after inclusion of the barrier, were about 3.5 cm less than the corresponding two-dimensional model elevations.

The next section describes both the two- and three-dimensional model equations used to numerically solve for the tidal elevations and velocities. This section is followed by the model results (section 3) for the existing tidal elevations, velocities, and frictional dissipation, followed by the results of placing an impermeable barrier across the narrow channel entering Minas Basin in the upper Bay of Fundy. The discussion (section 4) follows the results and is arranged in the same order of topics as the results section: elevations, velocities, frictional dissipation, and effects of a tidal barrier. Section 5 provides conclusions, and section 6 recommendations for future research.

2. Model equations

For the purpose of intermodel comparison, a two-dimensional and three-dimensional tide model was applied to the Gulf of Maine. The two-dimensional model used was a conventional finite-difference solution of the vertically averaged equations of motion on a staggered rectangular grid. The three-dimensional model used a sigma coordinate system in the vertical and an expansion of orthogonal cosine functions to approximate the vertical variation of horizontal velocities. The method used for the three-dimensional model is based on a formulation by Davies (1986) with some alterations to the treatment of the nonlinear convective terms in the momentum equations. The equations of motion used in the formulation of each model as well as a brief description of the three-dimensional model formulation are shown below. For a more complete description of the numerical technique used to solve the two-dimensional equations, the reader is referred to Greenberg (1977, 1983). A description of the application of this same finite-difference technique to the solution of the three-dimensional model equations is found in Cooper and Pearce (1977) and Pearce and Cooper (1981).

a. Two-dimensional model equations

The depth-averaged equations of motion used for the two-dimensional tide model are:

$$\frac{\partial \eta}{\partial t} + \frac{\partial[(H+\eta)U]}{\partial x} + \frac{\partial[(H+\eta)V]}{\partial y} = 0, \quad (1)$$

$$\frac{\partial U}{\partial t} + U\frac{\partial U}{\partial x} + V\frac{\partial U}{\partial y} - fV = -g\frac{\partial \eta}{\partial x} - \frac{kU\sqrt{U^2+V^2}}{(H+\eta)} + A_H\nabla^2 U, \quad (2)$$

$$\frac{\partial V}{\partial t} + U\frac{\partial VU}{\partial x} + V\frac{\partial V}{\partial y} + fU = -g\frac{\partial \eta}{\partial y} - \frac{kV\sqrt{U^2+V^2}}{(H+\eta)} + A_H\nabla^2 V. \quad (3)$$

In the preceding equations:

$\eta = \eta(x, y, t)$	the deviation of the free surface from mean sea level (m),
$H = H(x, y)$	the undisturbed water depth (m),
$U = U(x, y, t)$	the depth-averaged velocity in the x direction (m s^{-1}),
$V = V(x, y, t)$	the depth-averaged velocity in the y direction (m s^{-1}),
$f = f(y)$	the Coriolis parameter (s^{-1}),
g	the acceleration due to gravity (m s^{-2}),
k	the quadratic bottom friction factor (dimensionless),
$A_H = A_H(x, y, t)$	the horizontal eddy viscosity coefficient (m^2 s^{-1}).

The horizontal eddy viscosity coefficient was further parameterized as $A_H = 0.5a\Delta xH$, where a, the reduced horizontal eddy viscosity coefficient, is a constant. This formulation of horizontal eddy viscosity is used by both Greenberg (1983) and Schwiderski (1980).

b. Three-dimensional model equations

The three-dimensional tide model used for this study was a spectral-type model using the Galerkin method

to separate the depth-averaged flow equations from the equations that determine the velocity structure in the vertical. The set of equations is linked through bottom friction. The numerical technique is an extension of the earlier work of Pearce et al. (1979) and Pearce and Cooper (1981) coupled with a method developed by Davies (1986) for separating the external (vertically averaged) and internal (vertically varying) components of the flow. In addition we follow the work of Lardner and Cekirge (1988) in the sense that the advective terms in the momentum equations are retained only for the vertically averaged mode. This last simplification provides a savings in computer time over the fully developed nonlinear equations. For the Gulf of Maine, this simplification altered the numerical solution of the M_2 tidal amplitudes less than 1/4% as compared to a numerical solution that retained these terms. The equations used for the three-dimensional model are the three-dimensional shallow-water equations (Gill 1982):

$$\frac{\partial \eta}{\partial t} + \frac{\partial[(H+\eta)U]}{\partial x} + \frac{\partial[(H+\eta)V]}{\partial y} = 0, \quad (4)$$

$$\frac{\partial u}{\partial t} + u\frac{\partial u}{\partial x} + v\frac{\partial u}{\partial y} - fv = -g\frac{\partial \eta}{\partial x} + N_v\frac{\partial^2 u}{\partial z^2} + A_H\left(\frac{\partial^2 u}{\partial x^2} + \frac{\partial^2 u}{\partial y^2}\right), \quad (5)$$

$$\frac{\partial v}{\partial t} + u\frac{\partial v}{\partial x} + v\frac{\partial v}{\partial y} + fu = -g\frac{\partial \eta}{\partial y} + N_v\frac{\partial^2 v}{\partial z^2} + A_H\left(\frac{\partial^2 v}{\partial x^2} + \frac{\partial^2 v}{\partial y^2}\right). \quad (6)$$

The equation variables are as defined for the 2D model, and in addition,

$u = u(x, y, z, t)$ the horizontal velocity in the x direction (m s^{-1}),
$v = v(x, y, z, t)$ the horizontal velocity in the y direction (m s^{-1}),
$N_v = N_v(x, y, t)$ the vertical eddy viscosity coefficient (m^2 s^{-1}).

The depth-averaged currents U and V are related to u and v by

$$U = \frac{1}{D}\int_{-H}^{\eta} u\,dz, \quad V = \frac{1}{D}\int_{-H}^{\eta} v\,dz, \quad (7a,b)$$

where $D = H + \eta$, the total depth of the water column.

Bottom and surface boundary conditions are required along with Eqs. (4)–(6). The appropriate boundary conditions for the case of no wind stress at the surface are:

$$\rho N_v\frac{\partial u}{\partial z} = 0, \quad \rho N_v\frac{\partial v}{\partial z} = 0 \quad \text{at} \quad z = \eta \text{ (surface), and} \quad (8a,b)$$

$$-\rho N_v\frac{\partial u}{\partial z} = \tau_{bx}, \quad -\rho N_v\frac{\partial v}{\partial z} = \tau_{by} \quad \text{at} \quad z = -H \text{ (bottom).} \quad (9a,b)$$

A quadratic bottom stress relation is used with bottom stress related to the bottom velocity as

$$\tau_{bx} = -ku_b\sqrt{u_b^2 + v_b^2}, \quad \tau_{by} = -kv_b\sqrt{u_b^2 + v_b^2}. \quad (10a,b)$$

Relating (10) with (9) gives, as the final bottom boundary condition,

$$N_v\frac{\partial u}{\partial z} = ku_b\sqrt{u_b^2 + v_b^2}, \quad N_v\frac{\partial v}{\partial z} = kv_b\sqrt{u_b^2 + v_b^2}, \quad \text{at} \quad z = -H. \quad (11a,b)$$

The equations of motion and surface and bottom boundary conditions were transformed to a sigma coordinate system. This transformation of the z coordinate simplifies the solution of the equations by the Galerkin method. The new vertical coordinate, σ in terms of z, is

$$\sigma = \frac{H+z}{H+\eta} = \frac{H+z}{D}. \quad (12)$$

This relation maps the variable interval $[-H, \eta]$ into the constant interval [0, 1].

The transformation of the vertical coordinate to a fixed interval facilitates the evaluation of integrals that arise from the use of the Galerkin technique for numerically solving the momentum equations. The mapping complicates the original momentum equations; however, additional terms involving the partial derivative of the velocity component with respect to sigma arise. Nihoul (1982) has shown by order of magnitude arguments that for large coastal seas these new terms are small compared to the acceleration terms $\partial u/\partial t$ and $\partial v/\partial t$. In the present study, we numerically estimated the values of these terms at a location in the upper Bay of Fundy where these nonlinear terms would be greatest. These terms were at least two orders of magnitude less than the vertically averaged convective acceleration terms and thus were neglected for subsequent model calculations. The momentum equations were thus simplified to

$$\frac{\partial u}{\partial t} + u\frac{\partial u}{\partial x} + v\frac{\partial u}{\partial y} - fv = -g\frac{\partial \eta}{\partial x} + \frac{N_v}{D^2}\frac{\partial^2 u}{\partial \sigma^2} + A_H\left(\frac{\partial^2 u}{\partial x^2} + \frac{\partial^2 u}{\partial y^2}\right), \quad (13)$$

$$\frac{\partial v}{\partial t} + u\frac{\partial v}{\partial x} + v\frac{\partial v}{\partial y} + fu = -g\frac{\partial \eta}{\partial y} + \frac{N_v}{D^2}\frac{\partial^2 v}{\partial \sigma^2} + A_H\left(\frac{\partial^2 v}{\partial x^2} + \frac{\partial^2 v}{\partial y^2}\right), \quad (14)$$

which are nearly identical to the original nontransformed momentum equations (5) and (6) except the

vertical friction term is reduced by a factor of the total depth squared as the vertical derivative is now with respect to σ.

The Galerkin technique can now be applied to the momentum equations (13) and (14) to separate these equations into a vertically averaged mode and a series of higher modes that determine the vertical structure of the horizontal currents (Davies 1986). For this study we have retained only the vertically averaged part of the convective acceleration terms. Calculations of tidal elevations in the Gulf of Maine were made both with and without the convective terms added to the higher modes. The additional terms had a negligible effect on model elevations and velocities. In the larger Gulf of Maine changes to tidal amplitudes were of less than 1 millimeter with the additional terms. The largest change in model amplitude occurred in the upper Bay of Fundy where a difference of 8 mm was observed, representing a net change of less than 1/4%.

The separation of the momentum equations into modes is accomplished by writing the depth-dependent horizontal velocity components u, v as expansions of a set of basis functions f. Then

$$u(x, y, \sigma, t) = \sum_{I=1}^{N} c_I(x, y, t) f_I(\sigma),$$

$$v(x, y, \sigma, t) = \sum_{I=1}^{N} d_I(x, y, t) f_I(\sigma). \quad (15a,b)$$

For this study, $f_I = \cos[a_I(1 - \sigma)]$, where $a_I = 0, \pi, 2\pi, 3\pi, \cdots, (I-1)\pi$, for $I = 1, N$. With this choice of basis functions the first coefficient in the velocity expansions represents the vertically averaged velocity, since

$$U = \int_0^1 u d\sigma = c_1$$

and

$$V = \int_0^1 v d\sigma = d_1. \quad (16a,b)$$

Substituting the velocity expansions (15a,b) into the x momentum equation (13) and applying the Galerkin technique gives for the x momentum equation:

$$\int_0^1 \frac{\partial}{\partial t}\left(\sum_{I=1}^{N} c_I f_I\right) f_k d\sigma + \int_0^1 \left(\sum_{I=1}^{N} c_I f_I\right) \frac{\partial}{\partial x}\left(\sum_{J=1}^{N} c_J f_J\right) f_k d\sigma + \int_0^1 \left(\sum_{I=1}^{N} d_I f_I\right) \frac{\partial}{\partial y}\left(\sum_{J=1}^{N} c_J f_J\right) f_k d\sigma$$
$$- f \int_0^1 \left(\sum_{I=1}^{N} d_I f_I\right) f_k d\sigma = -g \frac{\partial \eta}{\partial x} \int_0^1 f_k d\sigma + A_H \int_0^1 \left[\frac{\partial^2}{\partial x^2}\left(\sum_{I=1}^{N} c_I f_I\right) + \frac{\partial^2}{\partial y^2}\left(\sum_{I=1}^{N} c_I f_I\right)\right] f_k d\sigma$$
$$+ \frac{N_v}{D^2} \int_0^1 \frac{\partial^2 u}{\partial \sigma^2} f_k d\sigma, \; k = 1, 2, 3, \cdots, N. \quad (17)$$

The last integral on the right-hand side is integrated by parts (Davies 1986) to obtain

$$\frac{N_v}{D^2} \int_0^1 \frac{\partial^2 u}{\partial \sigma^2} f_k d\sigma = -\frac{k u_b \sqrt{u_b^2 + v_b^2}}{D} f_k(0)$$
$$- \frac{N_v}{D^2} \int_0^1 \left(\sum_{I=1}^{N} c_I f'_I\right) f'_k d\sigma, \quad (18)$$

where the primes denote a partial derivative with respect to σ. The surface and bottom boundary conditions are thus explicitly entered into the model formulation.

The second and third terms in (17) represent the convective acceleration terms and now involve double summation of the model variables inside the integrals. Unlike the other terms of (17) these integrals cannot be simplified to contain only variables of a single mode. Retaining the complete set of convective acceleration terms dramatically increases computer time. An alternative, however, is to retain only the vertically averaged part of these terms. This simplification was also used by Lardner and Cekirge (1988) for their vertical/horizontal splitting model, which uses a conventional two-dimensional solution of tidal elevations as forcing for a solution of two horizontal momentum equations that determine the vertical structure of the flow.

The momentum equations thus simplify to a set of N equations involving successive time derivatives of the coefficients c_k, for $k = 1, 2, \cdots, N$. For $k = 1$, the Galerkin equation (17) becomes

$$\frac{\partial c_1}{\partial t} + c_1 \frac{\partial c_1}{\partial x} + d_1 \frac{\partial c_1}{\partial y} - f d_1 = -g \frac{\partial \eta}{\partial x}$$
$$- \frac{k u_b \sqrt{u_b^2 + v_b^2}}{D} + A_H\left(\frac{\partial^2 c_1}{\partial x^2} + \frac{\partial^2 c_1}{\partial y^2}\right), \quad (19)$$

which is nearly identical to the vertically averaged momentum equation (2) with the important exception that the bottom stress is determined from the calculated three-dimensional bottom velocity (u_b) instead of the vertically averaged velocity. (Recall that $c_1 = U$, the vertically averaged velocity.)

For $k = 2, 3, \cdots, N$, (17) simplifies to

$$\frac{\partial c_k}{\partial t} - fd_k = -\frac{2ku_b\sqrt{u_b^2 + v_b^2}\cos(a_k)}{D} - \frac{N_v a_k^2}{D^2} c_k \quad (20)$$

and represents the equations determining the velocity structure in the vertical. Here we have neglected the horizontal eddy viscosity term in the higher modes. This term could easily have been retained, but a numerical experiment on the Gulf of Maine with this term included did not alter the elevations to the accuracy of the model output of 1 mm. It is interesting to note that the higher modes are not directly affected by the external pressure gradient, but are forced instead by the bottom friction term. The last term of (20) represents frictional losses to internal dissipation.

The analogous set of equations for the y momentum equation are

$$\frac{\partial d_1}{\partial t} + c_1\frac{\partial d_1}{\partial x} + d_1\frac{\partial d_1}{\partial y} + fc_1 = -g\frac{\partial \eta}{\partial y} - \frac{kv_b\sqrt{u_b^2 + v_b^2}}{D} + A_H\left(\frac{\partial^2 d_1}{\partial x^2} + \frac{\partial^2 d_1}{\partial y^2}\right), \quad (21)$$

$$\frac{\partial d_k}{\partial t} + fc_k = -\frac{2kv_b\sqrt{u_b^2 + v_b^2}\cos(a_k)}{D} - \frac{N_v a_k^2}{D^2} d_k, \quad k = 2, 3, \cdots, N. \quad (22)$$

c. *Three-dimensional numerical scheme*

The common explicit leapfrog scheme used to solve the two-dimensional equations was also used to solve the momentum equations (19)–(22) along with the continuity equation (4) using the same staggered finite-difference grid. The additional bottom velocities required, u_b and v_b, are determined from the velocity expansions (15a,b) with $\sigma = 0$. Then,

$$u_b(i, j, t) = \sum_{I=1}^{N} c_I(i, j, t)\cos(a_I)_i$$

$$v_b(i, j, t) = \sum_{I=1}^{N} d_I(i, j, t)\cos(a_I). \quad (23a,b)$$

In all other respects the conventional two-dimensional numerical technique can be extended to solve the three-dimensional set of equations (Pearce and Cooper 1981).

3. Results for Gulf of Maine tide model

The three-dimensional and two-dimensional tide models were used to simulate the existing M_2 tide in the Gulf of Maine. For this purpose, the Gulf of Maine was divided into 120 × 120 grid cells. The grids were oriented along latitude and longitude lines and had dimensions of 3′ latitude in the north (y) direction and 4′ longitude in the east (x) direction. This grid division produces a Δx of $\approx$5 km and a Δy of $\approx$5.5 km. Depths were taken from various navigational charts at the center of each grid. Figure 1 shows the Gulf of Maine bathymetry and geometry as modeled with this resolution. The figure shows the shallows of Georges Bank and Browns Bank enclosing the interior Gulf of Maine with the only deep entrance from the Atlantic Ocean through the Northeast Channel. Three deep basins within the gulf are also clear: Georges Basin directly to the north of Georges Bank, Jordan Basin farther to the north, and Wilkinson Basin to the west.

The models were forced by specifying the elevation of the M_2 tide along the 400-m-depth contour at the shelf break. The M_2 amplitude and phase data were obtained from Moody (1984) and linearly interpolated along the model boundary where no data existed. The simple interpolation of the data along the model boundary is felt to be sufficiently accurate because the M_2 tide is essentially in phase and of nearly constant amplitude along the edge of the Northeast continental shelf of North America. There are only minor deviations in M_2 amplitude and phase along the 400-m contour of the model open boundary.

The models were independently tuned by adjusting the bottom friction factor, horizontal eddy viscosity coefficient, and vertical eddy viscosity coefficient (for the three-dimensional model only) to obtain an acceptable fit of M_2 amplitude and phase at 45 locations of known amplitude and phase. Thirty-eight of these locations were taken from Moody (1984), and 7 locations in the upper Bay of Fundy were taken from Greenberg (1977). Tidal velocity data at nine locations were also used to tune the three-dimensional model, particularly with respect to modeling the phase lag between surface and bottom currents. Parameters common to both models were $g = 9.81$ m s^{-2}, $\rho = 1025$ kg m^{-3}, and $\Delta t = 60$ s.

For the two-dimensional model the quadratic bottom friction parameter was 0.002. The reduced horizontal eddy viscosity coefficient a was 0.012. This value for a gives horizontal eddy viscosity coefficients in the range of 10^2 to 10^4 m^2 s^{-1} with a typical value (at 100-m depth) of approximately 3×10^3 m^2 s^{-1}.

The quadratic bottom friction parameter used for the three-dimensional model was 0.006, and the reduced horizontal eddy viscosity coefficient was 0.018. Horizontal eddy viscosity coefficients for the three-dimensional model were thus 50% larger than for the two-dimensional model. The vertical eddy viscosity coefficient was 0.07 times the square of the vertically averaged velocity, and so varied accordingly in horizontal space and time. Parameterizing the vertical eddy viscosity coefficient as a function of velocity squared is dimensionally consistent, as shown by Prandle (1982). The resultant values for vertical eddy viscosity coefficients compare well with values estimated from a relation by Csanady (1976) used by Garrett et al. (1978) to estimate tidal mixing in the Gulf of Maine. Wright and Loder (1985) used vertical eddy viscosity coefficients of 0.0185–0.0353 m^2 s^{-1} for a model of

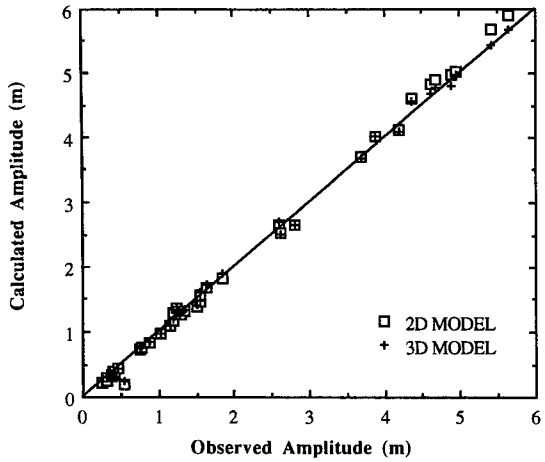

FIG. 2. Correlation between calculated and observed M_2 amplitudes for both 2D and 3D models.

tidal rectification over Georges Bank. These values compare to the range 0.0175–0.0360 $m^2 s^{-1}$ in the same region for the present model. Finally, ten cosine functions were used to approximate the vertical variation of velocity.

a. *Comparison of model amplitudes and phases to data*

Figures 2 and 3 show the correlation between observed and calculated M_2 amplitude and phase, respectively, for both the two-dimensional and three-dimensional models. A perfect match with data, then, would lie along the line $y = x$. The station names, designated number, elevation data, and corresponding model calculations for the 45 stations from which these plots were constructed are listed in the Appendix. The M_2 component of the model tidal elevations was determined using a NOAA harmonic analysis program by Dennis and Long (1978). Figure 4 shows the geographical location of each of the 45 stations used for comparison by designated number.

In general, the model elevations were accurate to within 10% of amplitude and 20° of phase with a few exceptions. The greatest errors for amplitude occurred at stations to the west of Georges Bank over Nantucket Shoals where the gradient of the coamplitude and cophase lines of the M_2 tide are relatively steep (Fig. 5). Errors due to model grid scale are likely to be important in this region where relatively large changes in amplitude and phase occur across a single grid. Additionally, this area contains an amplitude minimum with amplitudes less than 30 cm. Absolute errors in amplitude thus produce much greater percent errors compared to the same absolute errors in the interior of the Gulf of Maine where the amplitudes are some five times or more larger.

The rms error of amplitudes and phases for all 45 locations in the Gulf of Maine and Bay of Fundy was 7.9 cm and 6 deg for the two-dimensional model and 5.7 cm and 7 deg for the three-dimensional model. The greater overall accuracy for the three-dimensional model for amplitudes is due to slightly greater accuracy for stations in the upper Bay of Fundy. Overall rms error, however, is not an indication that the three-dimensional model was more accurate then the two-dimensional model because of the relatively poor model resolution in the upper Bay of Fundy. The rms error for both models, omitting stations 39–45 in the upper Bay of Fundy and stations 10–16 on Nantucket Shoals, was 5.0 cm in amplitude and 5 deg in phase for the two-dimensional model and 4.9 cm in amplitude and 5 deg in phase for the three-dimensional model.

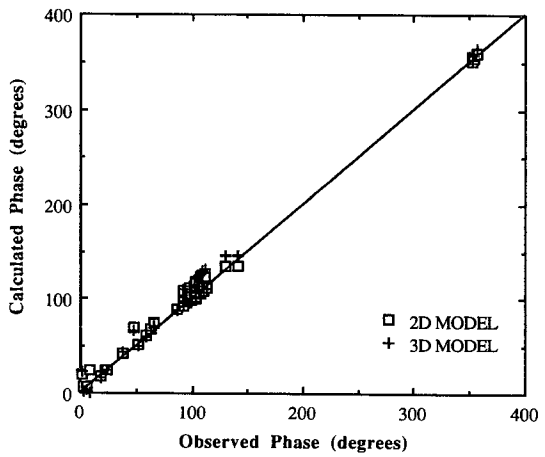

FIG. 3. Correlation between calculated and observed M_2 phases for both 2D and 3D models.

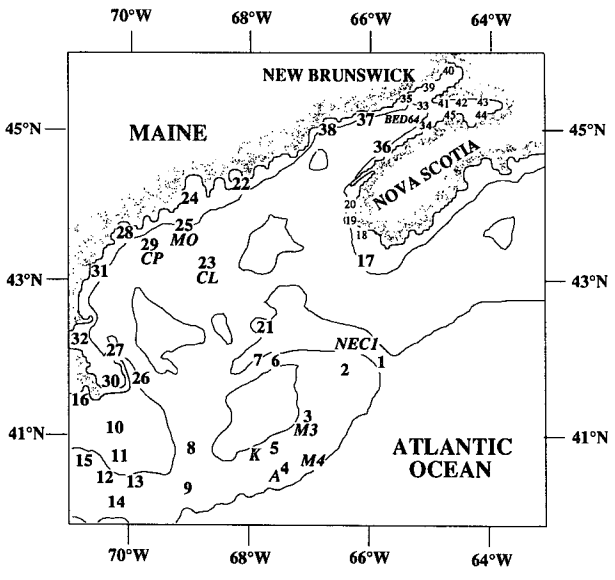

FIG. 4. Locations of stations used for model tuning and comparison. Numbered stations (1–45) are locations of M_2 elevation data and italicized lettered stations are locations of velocity data. Location names for numbered stations are listed in the Appendix.

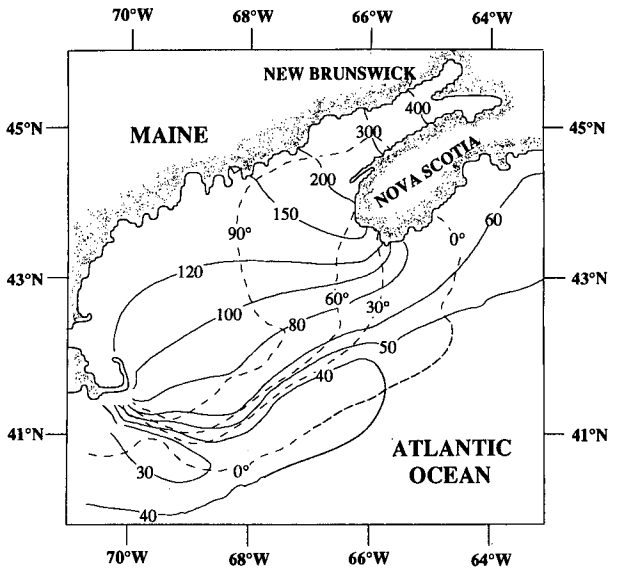

FIG. 5. Coamplitude (cm) and cophase (degrees) lines of the M_2 tide as calculated by the three-dimensional model.

The arithmetic difference of amplitudes and phases between the two- and three-dimensional models is contoured in Figs. 6 and 7, respectively. For these and all subsequent plots of model differences, we have taken *difference* = 2D model data − 3D model data, so that a positive value of *difference* represents a greater value for the two-dimensional model. Figures 6 and 7 show that the M_2 tide calculations for the two models generally agree to within 3 cm of amplitude and 3 deg of phase. The greater differences between the models are found for the Nantucket Shoals, the upper Bay of Fundy, and the Nova Scotia side of the mouth of the Bay of Fundy where amplitude and phase differences reach 10 cm and 10 deg.

A contour plot of M_2 amplitudes and phases calculated from the three-dimensional model is shown in Fig. 5. This plot can be compared with available contour plots of the region as constructed from data, such as that found in Moody et al. (1984). The model-constructed coamplitude and cophase lines in Fig. 5 represent the features of the M_2 tide in the Gulf of Maine well. The model correctly shows the amplitude minimum of less than 30 cm over Nantucket Shoals, the convergence of co-amplitude and co-phase lines to the south of Cape Cod, the broad separation of the 50- and 60-cm amplitude contours south of Nova Scotia, the bending of the 120-cm amplitude contour toward the Maine coast, and the rapid increase in amplitude towards the head of the Bay of Fundy. The model also correctly shows the rapid change in phase around the western side of Nova Scotia, and the sharp hook of the 90-deg phase contour to the north of Georges Bank.

Table 1 compares amplitudes and phases from the two- and three-dimensional models to the 1977 Greenberg model at 19 stations common to both model studies. The Greenberg model is generally more accurate than either of the two models used for this study, which we attribute to Greenberg's greater model resolution in the Bay of Fundy.

b. Comparison of model velocities to data

Model velocities were compared to data at nine locations throughout the model area. These data were also taken from Moody (1984). The approximate location of each station, indicated by the italicized station name, is shown in Fig. 4.

We used a simple numerical integration to estimate average velocity at each station. These estimates may be somewhat crude because of the lack of velocity measurements with depth at some stations. Brown (1984), however, made average velocity estimates at stations CP, MO, CL, M3, and M4 based upon estimates of the velocity profiles at each station. Brown's average velocity estimates compared well with our own, and for station M3, where only one depth location was available, we used Brown's estimate of the vertically averaged velocity directly.

Table 2 compares the observed vertically averaged, east and north component of the M_2 current with the corresponding results from both the two- and three-dimensional model. Table 3 compares the observed components of M_2 velocity at each depth where data were available with the calculated velocity from the three-dimensional model for the nine stations. The M_2 component of the model velocities was determined using a NOAA harmonic analysis program by Dennis and Long (1978).

Model-calculated vertically averaged velocities differed from observed values by no more than 3 cm s^{-1}

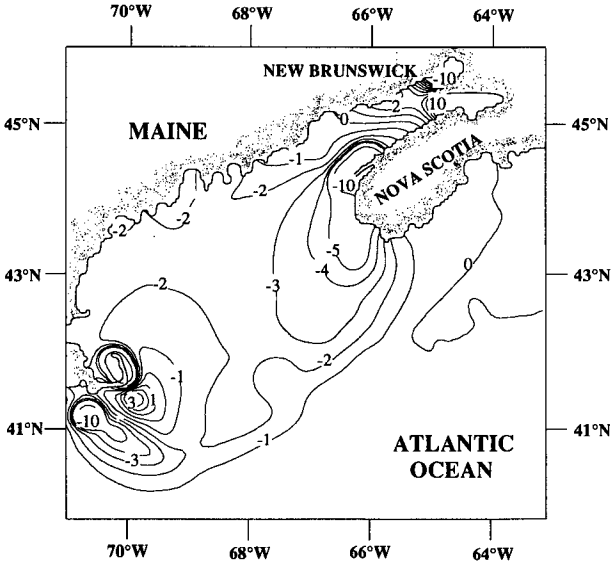

FIG. 6. The M_2 amplitude differences (cm) between 2D and 3D models. Positive values of difference are greater for the 2D model.

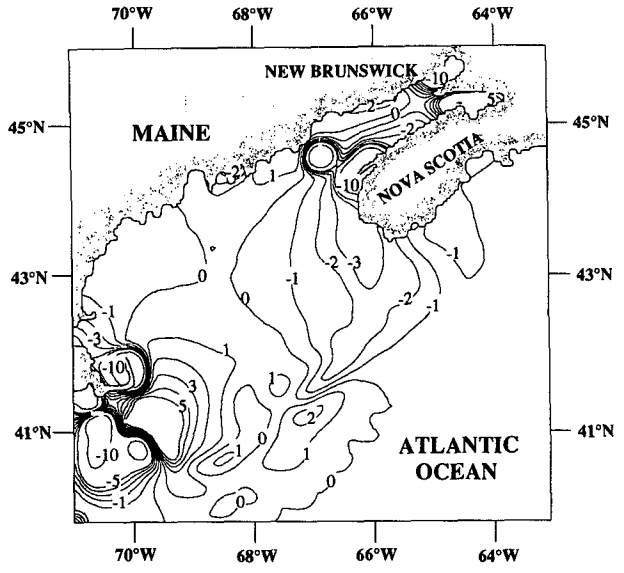

FIG. 7. The M_2 phase differences (degrees) between 2D and 3D models. Positive values of difference are greater for the 2D model.

at all stations except BED64 in the Bay of Fundy, where model velocities were about 10% higher than observed. The rms error for averaged velocity amplitude and phase, regardless of direction, was 3 cm s^{-1} and 7 deg for the two-dimensional model and 3 cm s^{-1} and 9 deg for the three-dimensional model. The greater velocity at BED64 is consistent with the overestimate of model elevations in the upper Bay of Fundy. The similarity between the two models for vertically averaged velocity is expected, given the modest differences in model elevations. Continuity of volume dictates that the averaged velocities will be correspondingly similar.

The comparisons of the observed velocity structure to three-dimensional model velocities in Table 3 show greater variability than the comparisons of averaged velocities, although the rms errors for velocity are a comparable 3.5 cm s^{-1} in amplitude and 10 deg in phase. In general, the three-dimensional model predicts essentially uniform velocity profiles with little change in phase at the deeper stations in the Gulf of Maine (CL, MO, and CP). The observational data, however, indicates considerably greater variability with depth particularly with respect to phase. At station NEC1, a deep-water station in the Northeast Channel, the model failed to show the large near-bottom amplitude of the northward component of the tidal velocity observed at 200-m depth. The model generally produced a good match with data at the shallower stations on Georges Bank (M4, A, K, and M3). The near-bottom velocity gradient at stations A and K is somewhat steeper than that predicted by the model, so that the model underestimates the velocity amplitude several meters above the bottom at those stations, while the velocity amplitudes 1 m above the seafloor are more accurate. This error is likely a numerical problem of approximating a steep curve with a limited set of cosine functions.

An important aspect of the velocity comparisons for the three-dimensional model was to model the phase lag between the vertically averaged and bottom current in order to have confidence in dissipation calculations. At stations M4, A, and K the model matched this difference to within 11° with an average error of 6 deg.

c. *Frictional dissipation*

The total frictional dissipation over a tidal cycle was calculated at each grid for both the two- and three-dimensional model. This calculation was done in order

TABLE 1. The M_2 amplitude (m) and phase (degrees) from observation and as calculated by Greenberg (1977) and the 2D and 3D models for stations common to the 1977 Greenberg model.

	Data		Greenberg model		2D model		3D model	
Station	Amplitude	Phase	Amplitude	Phase	Amplitude	Phase	Amplitude	Phase
17. Seal Island	1.20	52	1.24	44	1.29	52	1.35	50
18. Pinkney	1.55	59	1.52	59	1.55	62	1.61	60
19. Yarmouth	1.63	63	1.60	61	1.67	69	1.74	67
20. Port Maitland	1.85	66	1.85	69	1.83	74	1.90	72
22. Bar Harbor	1.55	93	1.60	89	1.46	93	1.50	93
24. Rockland	1.50	98	1.47	96	1.40	99	1.42	97
28. Portland	1.33	103	1.34	101	1.31	102	1.33	100
31. Portsmouth	1.30	107	1.29	102	1.27	105	1.29	103
32. Boston	1.35	111	1.33	109	1.32	108	1.34	111
34. Margaretville	3.87	92	3.88	94	4.02	108	4.01	110
36. Centreville	2.61	92	2.65	87	2.66	98	2.70	97
38. Eastport	2.61	99	2.67	91	2.54	105	2.50	107
39. Cape Enrage	4.36	104	4.38	102	4.60	118	4.56	123
40. Hopewell Cape	4.96	109	4.76	111	5.02	123	4.98	130
41. Port Greville	4.61	109	4.64	106	4.83	122	4.68	129
42. Dilligent River	4.88	112	4.81	111	4.98	124	4.82	131
43. Five Islands	5.42	130	5.42	135	5.68	134	5.44	146
44. Burntcoat Head	5.64	141	5.53	152	5.91	135	5.68	147
45. Scots Bay	4.67	106	4.68	107	4.89	119	4.77	126

TABLE 2. East and north M_2 components of observed vertically averaged velocity at nine locations and as calculated by the 2D and 3D models. Observed vertically averaged velocities were estimated by a simple numerical integration. Averaged velocity at station M4 is from Brown (1984).

	East amplitude (m s^{-1})			East phase (deg)			North amplitude (m s^{-1})			North phase (deg)		
Station	Data	2D model	3D model	Data	2D model	3D model	Data	2D model	3D model	Data	2D model	3D model
NEC1	0.40	0.40	0.41	157	175	173	0.36	0.33	0.33	13	22	20
CL	0.06	0.05	0.05	227	230	221	0.08	0.10	0.11	359	7	7
MO	0.04	0.03	0.03	312	303	303	0.06	0.07	0.07	13	6	5
BED64	0.80	0.90	0.89	22	36	44	0.48	0.59	0.59	26	34	41
M4	0.26	0.29	0.29	144	139	140	0.31	0.34	0.32	33	31	31
A	0.26	0.28	0.28	130	135	135	0.33	0.34	0.33	21	26	25
K	0.39	0.40	0.41	136	135	137	0.47	0.50	0.49	27	26	26
CP	0.02	0.03	0.03	234	218	212	0.04	0.06	0.05	336	348	348
M3	0.51	0.52	0.54	129	132	133	0.66	0.67	0.65	22	29	30

to determine whether or not there were any significant differences in the spatial distribution of frictional dissipation as modeled by the two different techniques. In addition, it was assumed that since the two models were tuned to produce nearly identical surface elevations, the total global model dissipation would be essentially the same for both models. The calculation of the model dissipation thus provides corroboration of this assertion.

The frictional dissipation associated with the bottom friction stress in each model is simply the dot product of the associated vector bottom stress and the total velocity. For the two-dimensional model the associated velocities used to determine the bottom friction dissipation were vertically averaged while the associated three-dimensional model velocities were at the bottom ($\sigma = 0$). The final quantity of dissipation rate had units of watts per square meter. The bottom frictional dissipation for the two-dimensional model at each grid is thus

$$\tau_b \cdot \mathbf{Q} = -k\rho(U^2 + V^2)^{3/2} \qquad (24)$$

TABLE 3. East and north M_2 components of velocity from observation and calculated by the 3D model at available depths. The mean depth of each station is indicated under the station designation in column 1.

Station and depth (m)	Depth of observation (m)	East amplitude (m s^{-1})		East phase (deg)		North amplitude (m s^{-1})		North phase (deg)	
		Data	3D model	Data	3D model	Data	3D model	Data	3D model
NEC1 233	103	0.42	0.44	162	175	0.33	0.34	18	24
	153	0.45	0.44	157	174	0.42	0.35	18	25
	207	0.28	0.29	141	164	0.41	0.29	350	351
CL 190	33	0.08	0.05	233	219	0.12	0.11	10	9
	68	0.06	0.05	240	220	0.07	0.11	16	8
	118	0.06	0.05	218	218	0.09	0.11	346	10
MO 98	33	0.04	0.03	287	303	0.08	0.07	356	5
	68	0.03	0.03	338	303	0.04	0.07	32	5
BED64 50	10	1.01	1.04	16	52	0.61	0.69	27	38
	25	0.86	0.95	25	45	0.51	0.62	25	42
M4 77	10	0.31	0.31	158	146	0.36	0.34	46	38
	36	0.29	0.32	151	143	0.33	0.36	41	36
	69	0.21	0.21	123	124	0.27	0.26	11	11
A 85	15	0.28	0.30	137	141	0.34	0.34	27	31
	45	0.29	0.31	134	138	0.36	0.36	26	29
	75	0.28	0.21	119	121	0.31	0.28	8	6
	84	0.14	0.12	108	116	0.21	0.17	360	356
K 61	10	0.44	0.51	142	142	0.51	0.57	34	34
	15	0.42	0.49	139	140	0.50	0.56	30	32
	34	0.44	0.44	142	136	0.51	0.53	34	26
	54	0.32	0.30	125	128	0.42	0.38	15	11
	58	0.30	0.21	129	126	0.39	0.28	19	6
	60	0.22	0.19	116	126	0.30	0.25	8	5
CP 98	33	0.03	0.03	228	212	0.06	0.05	334	348
	68	0.01	0.03	240	212	0.03	0.05	337	348
M3 44	36	0.47	0.40	129	130	0.55	0.50	22	23
	—	—	—	—	—	—	—	—	—

and for the three-dimensional model at each grid is

$$\tau_b \cdot \mathbf{q}_b = -k\rho(u_b^2 + v_b^2)^{3/2}. \quad (25)$$

The eddy viscosity terms also contribute to the total dissipation rate and were treated in an analogous manner as molecular viscosity in producing a dissipation rate, commonly designated as ϵ (Gill 1982). The dissipation rate resulting from the horizontal eddy viscosity parameter at each grid is

$$\epsilon_{A_H} = \rho D A_H \left[\left(\frac{\partial U}{\partial x}\right)^2 + \left(\frac{\partial U}{\partial y}\right)^2 + \left(\frac{\partial V}{\partial x}\right)^2 + \left(\frac{\partial V}{\partial y}\right)^2\right]. \quad (26)$$

The analogous expression for the dissipation rate produced by the vertical eddy viscosity term in the three-dimensional model involves an integral over the depth in order to arrive at the dissipation associated with each grid. Rather than computing this integral numerically, however, the expression can be simplified by first substituting the cosine expansions (21a,b) for the three-dimensional velocities and then simplifying the resultant expression. The dissipation rate associated with the vertical eddy viscosity at each grid is then

$$\frac{\rho N_v}{D} \sum_{I=1}^{N} c_I^2 a_I^2 \int_0^1 \sin^2[a_I(1-\sigma)]\, d\sigma = \frac{\rho N_v}{2D} \sum_{I=2}^{N} c_I^2 a_I^2. \quad (27)$$

This final expression (37) was thus used to calculate the internal dissipation rate due to vertical eddy viscosity.

The dissipation rates were summed over both the Gulf of Maine and Bay of Fundy for both two- and three-dimensional models. The total dissipation rates averaged over one tidal cycle for the two-dimensional model were 1.1×10^{10} W for the Bay of Fundy and 3.8×10^{10} W for the Gulf of Maine. For the three-dimensional model, the corresponding dissipation rates were 1.2×10^{10} and 3.7×10^{10} for the Bay of Fundy and Gulf of Maine, respectively. Greenberg (1979) estimated corresponding average dissipation rates of 1.9×10^{10} and 3.6×10^{10} W from his two-dimensional nested grid model. The dissipation due to horizontal eddy viscosity represents 18% of the total dissipation for the two-dimensional model and 26% of the total dissipation for the three-dimensional model.

The calculated total average dissipation rate (W m^{-2} $\times 10^{-2}$) for the three-dimensional model is shown in Fig. 8. The features and magnitudes of the distribution of dissipation is essentially identical to that shown by Greenberg (1979) for his two-dimensional model. There are four primary areas of dissipation outside the Bay of Fundy. These are on Georges Bank, over Nantucket Shoals, off southwest Nova Scotia, and at the mouth of the Bay of Fundy.

The differences in dissipation rate between the two- and three-dimensional models are shown in Fig. 9. In this figure, positive numbers indicate greater dissipation rate for the two-dimensional model. This plot shows that the two-dimensional model produces greater dissipation on a broad area over much of Georges Bank. The three-dimensional model produces greater dissipation toward the north side of Georges Bank and extending along the steep slope into Georges Basin. The three-dimensional model also produces greater dissipation in the regions of large total dissipation mentioned before. It is tempting to speculate that greater tidal mixing might thus be predicted by the three-dimensional model in these regions, but we will show in section 4 that this is not likely to be the case.

d. Simulation of a tidal barrier

The effect of a tidal barrage in the upper Bay of Fundy was simulated by simply specifying a no-flow boundary condition through the narrows of Minas Basin. Thus, the entire Minas Basin was cut off from the Gulf of Maine. This barrier scenario corresponds to Greenberg's impermeable barrier case at Blomidon, and was found by Greenberg (1977) to produce the greatest increase to the tide in the Gulf of Maine among all barrier schemes tested. This idealized condition does not reflect changes to the tide that would result from the actual planned barrier scenario. As we are interested in the differences between the two- and three-dimensional models, and not the absolute effect of various barrier schemes on the tides, we chose the condition that resulted in the greatest alteration to the tides in the Greenberg study. Therefore, these results should be interpreted in this light and are not predictions of absolute amplitude alterations caused by the Tidal Power Corporation's proposed barrier schemes. These model results should also not be used for estimating quantitative changes to the tide because of the lack of grid resolution in the upper Bay of Fundy.

The inclusion of the barrier in Minas Channel resulted in an increase in tidal amplitudes throughout the model region for both the two- and three-dimensional models. Both models predict an increase of 30–50 cm in amplitude in the Gulf of Maine. Contours of amplitude increases for both the three- and two-dimensional models are shown in Figs. 10 and 11, respectively. The two-dimensional model predicts slightly greater amplitudes throughout the Gulf of Maine than the three-dimensional model, although the spatial features of the response are similar. The three-dimensional model predicted greater amplitude increases in the upper Bay of Fundy than the two-dimensional model. The differences in amplitude increase between the models are shown in Fig. 12, where positive values indicate greater amplitude changes for the two-dimensional model. This plot shows that the two-dimensional model produced greater amplitude differences over the entire Gulf of Maine, outside of the Bay of Fundy, but these differences were nowhere greater than 4 cm.

Table 4 compares pre- and postbarrier amplitudes

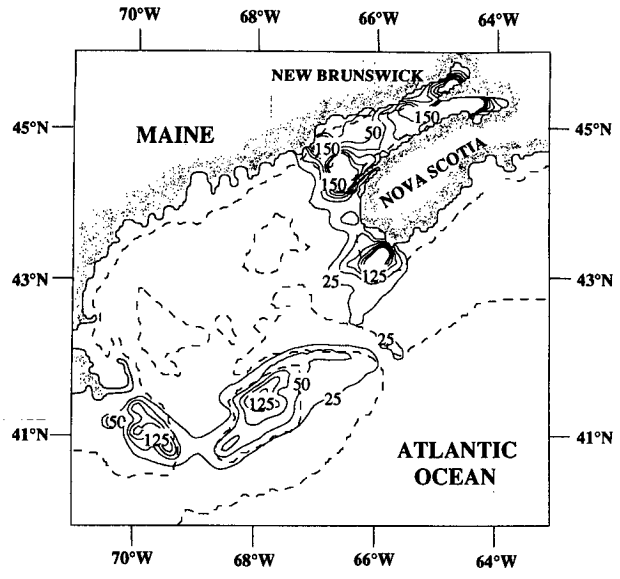

FIG. 8. Total M_2 dissipation rate (W $m^{-2} \times 10^{-2}$) averaged over a tidal cycle for the 3D model. Dashed lines indicate the 50-m and 200-m depth contour. Total average dissipation rate summed over the entire grid was 4.9×10^{10} watts.

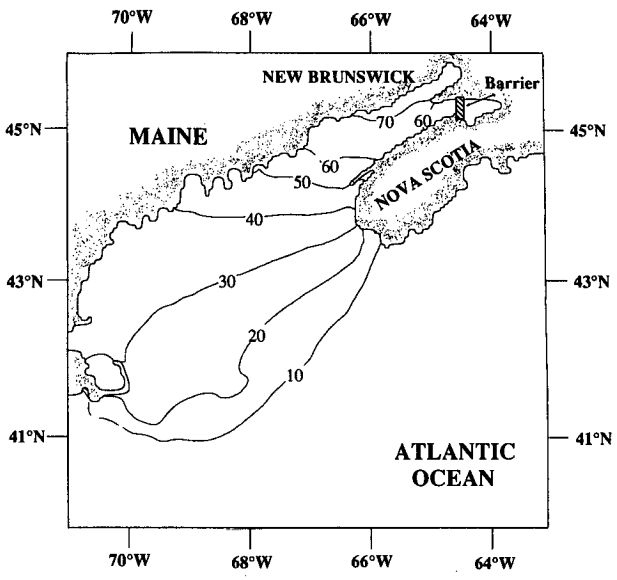

FIG. 10. Change in M_2 amplitudes (cm) after inclusion of impermeable barrier in upper Bay of Fundy as predicted by 3D model.

at four stations as predicted by the 1977 Greenberg model (impermeable, Blomidon barrier), and the two- and three-dimensional models of this study.

4. Discussion

a. Elevations

The two- and three-dimensional models performed equally well in replicating the tide in the Gulf of Maine, as is evident from the correlation plots of observed and calculated model amplitudes and phases (Figs. 2 and 3). Neither model achieved the overall accuracy of the 1977 Greenberg model and we attribute this to the better grid resolution of the Greenberg model in the Bay of Fundy. The Greenberg model had a grid resolution of approximately 2 km in the Bay of Fundy compared to 5 km in the present study. Other model studies have documented the importance of grid scale in the upper Bay of Fundy as well as the importance of including the extensive sandflat regions there

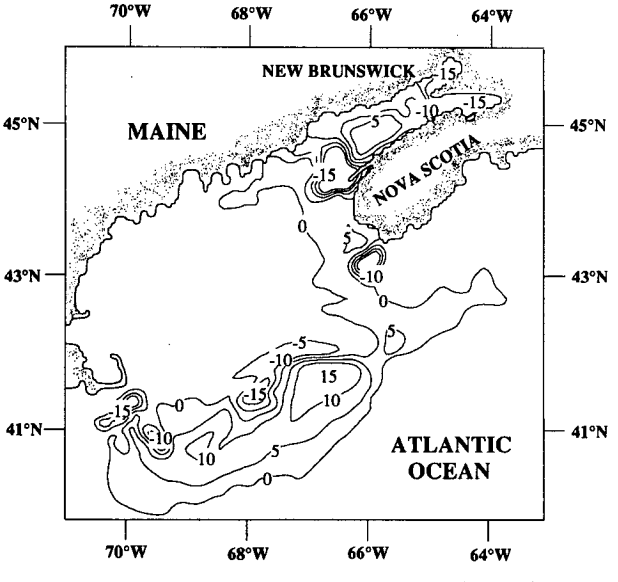

FIG. 9. Difference in M_2 dissipation rates (W $m^{-2} \times 10^{-2}$) for 2D and 3D models. Positive values indicate greater dissipation for 2D model.

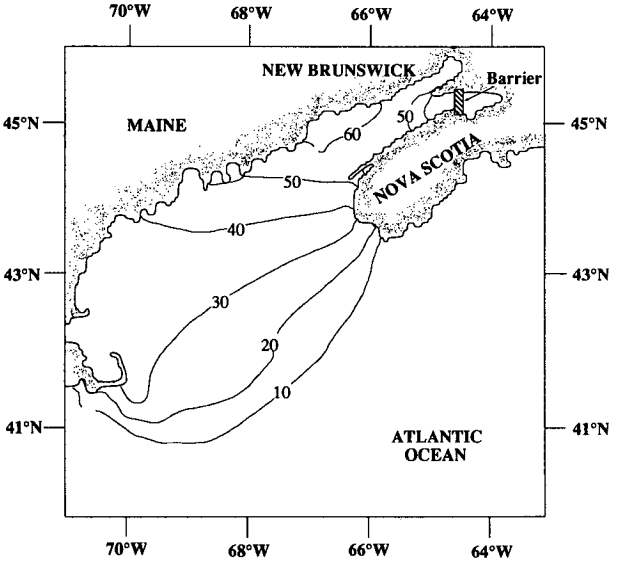

FIG. 11. Change in M_2 amplitudes (cm) after inclusion of impermeable barrier in upper Bay of Fundy as predicted by 2D model.

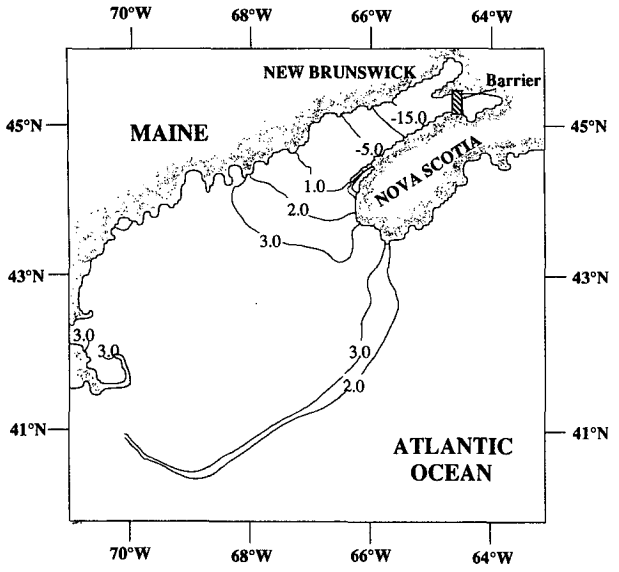

FIG. 12. Difference in M_2 amplitude changes (cm) caused by barrier for 2D and 3D models. Positive values indicate greater postbarrier increase of amplitude for 2D model.

(Greenberg 1983; Duff 1981). The fact that both the present models, despite having fundamentally different ways of approximating friction, behaved in essentially the same fashion for the Gulf of Maine also indicates that for M_2 tidal prediction in the gulf attention to bathymetry and geometry are extremely important. This result is not surprising as bathymetry and geometry are fundamental to modeling free period, which in turn determines the degree of proximity of the M_2 tidal forcing to resonance.

b. *Velocities*

The two- and three-dimensional models produced nearly identical average velocities (Table 2) and both compared well with data. This result is a consequence of the two models producing similar results for elevation.

The three-dimensional model showed greater variability in matching observed velocities at individual depths than for matching average velocity. In general, the model produced a closer match with data for the shallower stations over Georges Bank, than for the deeper stations in the interior of the Gulf of Maine. For the deeper stations, the model predicted virtually uniform velocity profiles with little change in phase with depth while the observations indicate considerably more variability with depth, particularly with respect to phase. This result could be explained by the greater extent of stratification at the deeper stations for which the model takes no account. Greater stratification would decrease the value of the eddy viscosity coefficient at these locations which would increase the vertical structure of the velocities by reducing damping of the higher modes. Vertical structure could also be increased by increasing the bottom friction, however, as this term damps the vertically averaged mode and forces the higher modes. Thus, a mechanism that increases bottom friction in these areas, such as the nonlinear interaction of relatively larger nontidal velocities near the bottom, could also explain the model mismatch with observation.

Based on an analytic solution for the vertical structure of tidal currents (Prandle 1982), we estimated that the vertical eddy viscosity coefficient would need to be reduced to 5×10^{-5} m^2 s^{-1} (from 1.75×10^{-4} m^2 s^{-1}) to approximate the observed vertical structure of the tide at the deep-water stations in the Gulf of Maine. This value for eddy viscosity is a reasonable reduction based on the eddy viscosity reduction factor of 0.3 (85 H^{-1}) used by Loder and Wright (1985) for Georges Bank.

David Brooks (personal communication) has noted the possible presence of internal waves of tidal frequency in the interior Gulf of Maine, which would produce velocity observations at the deeper stations for which the constant density model cannot account. The presence of internal waves could also explain the model mismatch with data at station NEC1 in the Northeast Channel, where the model underestimated the amplitude of the northward component of velocity at 207 m depth by 40%.

c. *Frictional dissipation*

The total dissipation rates averaged over a tidal cycle for the two models agreed to within 4%. Predicted total dissipation in the Gulf of Maine compares well with

TABLE 4. The M_2 amplitude (cm) of existing tide and of postbarrier tide as predicted by Greenberg (1977) and the 2D and 3D models. Percent increase in amplitude predicted by each model for each station is also shown.

		No barrier			With barrier			Percent change		
Station	Data	Greenberg model	2D	3D	Greenberg model	2D	3D	Greenberg model	2D	3D
Boston	134	133	132	134	172	165	165	29	25	23
Bar Harbor	155	160	146	150	198	200	199	24	37	33
Cape Enrage	436	430	460	456	470	505	523	7	10	15
Yarmouth	163	160	167	174	180	202	205	10	21	18

Greenberg (1979) [3.7–3.8 ($\times 10^{10}$) compared to 3.6 $\times$ 10^{10} W]. The total dissipation rates for the Bay of Fundy were less for the present models (1.1–1.2 ($\times 10^{10}$) compared to 1.9 $\times$ 10^{10} W). The discrepancy in the Bay of Fundy is, again, attributable to model resolution. For total dissipation over the entire system the two- and three-dimensional models differ by 2%. Total dissipation for the Greenberg model was 15% higher than the present models. The Greenberg model must then have a corresponding greater amount of work done across the open model boundary, which is an indication that the Greenberg model is in slightly greater resonance with the forced M_2 tide.

Areas of large tidal dissipation (Fig. 8) correspond with heavily mixed frontal areas observed by satellite (Yentsch 1981). The correlation between tidal dissipation rate and vertically well-mixed regions of the Gulf of Maine was noted by Garrett et al. (1978). The large dissipation rate across the mouth of the Bay of Fundy is of interest because this area contains a relatively deep passage of 200 m that extends into the Bay of Fundy from Jordan Basin and is an area of important upwelling of nutrient rich bottom waters into the photic zone (Townsend 1987).

As shown in Fig. 9, there were spatial variations in dissipation between the two models. In order to assess whether these variations would significantly alter predicted areas of vertical mixing, we calculated the difference between the two models for the parameter $\log(HD^{-1})$ used by Garrett et al. (1979). Here H represents depth and D dissipation in units of watts per square meter. Garrett showed that for the Gulf of Maine well-mixed regions are observed to occur for $\log(HD^{-1}) < 1.9$. Contours of the difference in this parameter for the models are shown in Fig. 13. This mixing parameter varies by up to 0.4 units but varies very little in the regions of high dissipation (Georges Bank, southwest Nova Scotia, and the mouth of the Bay of Fundy) where the 1.9 contour of $\log(HD^{-1})$ would occur. Only in a relatively small region just south of Cape Cod does the three-dimensional model predict a greater extent of well-mixed water.

d. Effect of a tidal barrier

An impermeable barrier placed across the channel into Minas Basin caused an increase in tidal elevations in the Gulf of Maine of roughly the same magnitude as predicted by Greenberg (1977) (Table 4). Table 4 shows that the two- and three-dimensional models of the present study predict amplitude changes within 10% of the changes predicted by the Greenberg model for the same barrier case. These minor differences between our results and the Greenberg model could be due to differences in grid scale, bathymetry, parameterization of friction etc., but it is clear that the Greenberg model and both our two- and three-dimensional model responded to a tide barrier in essentially the same way.

The comparison between the two- and three-dimensional model predictions was of greater interest. Here we had two models using identical grid resolution and bathymetry and tuned to match the existing tide with nearly identical precision. Differences in postbarrier amplitudes between the two- and three-dimensional models were assumed to be due to the differences in modeled physics.

The two- and three-dimensional model predicted very similar postbarrier elevations (Table 4). However, the three-dimensional model was uniformly less sensitive than the two-dimensional model to the addition of the barrier at locations outside the Bay of Fundy and more sensitive to the barrier inside the Bay of Fundy (Fig. 12). Still, at Boston the three-dimensional model predicted an increase of only 3 cm less than the two-dimensional model out of a total increase of about 30 cm.

5. Conclusions

Both a two- and three-dimensional tide model were used to simulate the existing M_2 tide in the Gulf of Maine. These models differ primarily in the specification of bottom friction with the three-dimensional model parameterizing bottom friction in a more realistic fashion as a function of the near-bottom velocity rather than the vertically averaged velocity. We found, however, that both models simulated the existing M_2 tide with nearly equal precision. There was no apparent advantage of the three-dimensional model over the two-

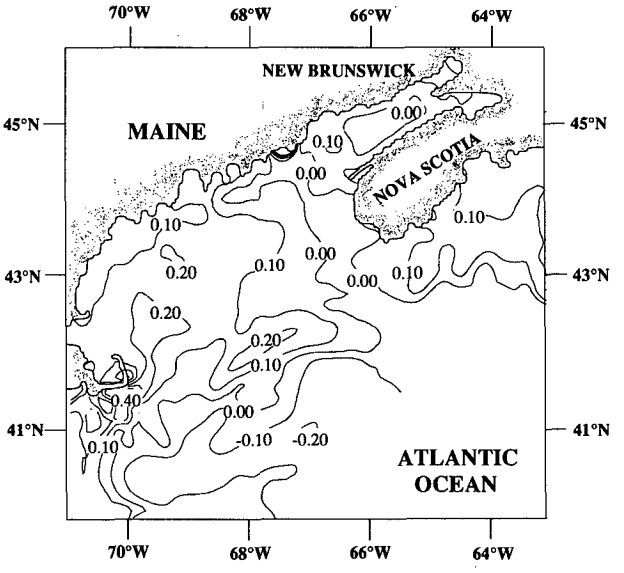

FIG. 13. Difference in vertical mixing parameter, $\log_{10}(H/D)$, for 2D and 3D models. There is generally good correlation between areas of well-mixed water and areas of mixing parameter less than 1.9 for the Gulf of Maine (Garrett et al. 1978). Negative values of difference here indicate more energy available for vertical mixing in the 3D model.

dimensional model for simulating either tidal amplitudes or average velocities. This result should not be taken as a generality for other tidal regions, as the Gulf of Maine is unique in its extreme resonance with the M_2 ocean tide. This physical situation means that numerical tide models of this region are more sensitive to bathymetry and geometry than for other regions and the importance of model friction is correspondingly reduced in overall importance. This is not to say that friction is not important, but only that overall model accuracy is more likely to be affected by bathymetric and geometric inaccuracies in the Gulf of Maine than in regions that are not dominated by extreme resonance (Sucsy 1990). Both models were generally less accurate for reproducing the existing tide than the 1977 Greenberg model. The greater accuracy of the Greenberg model is likely due to the finer grid resolution in the Bay of Fundy.

The total frictional dissipation rate averaged over a tidal cycle was calculated for each model. The calculated dissipation rates outside the Bay of Fundy compared well between the two models and with the Greenberg model, confirming that the tidal dissipation rates for the M_2 tide averaged over a tidal cycle are 3.6–3.8 ($\times 10^{10}$ W) for the Gulf of Maine.

The dissipation rate per tidal cycle did differ spatially for the two- and three-dimensional models by up to 0.15 W m^{-2} over large sections of the modeled area. This value represents up to 3750 megawatts per grid. The largest differences in dissipation rates between the two models also coincided with areas of large frictional dissipation over Georges Bank, east of Nantucket Island, off western Nova Scotia, and in the mouth of the Bay of Fundy. These regions are also associated with regions of tidal fronts (Yentsch 1981). The spatial differences in dissipation, however, were not significant enough to alter predictions of tidally mixed regions based upon the tidal mixing parameter used by Garrett et al. (1978).

Both models predicted an increase of tidal amplitude in the Gulf of Maine of 30–50 cm when an impermeable barrier was placed across the channel entering Minas Basin in the upper Bay of Fundy. This result corroborates the earlier Greenberg study (1977) for an impermeable barrier at Blomidon. There were small differences for amplitude changes between the two models of less than 4 cm in the Gulf of Maine. Differences in amplitude changes between the two models varied only slightly over the entire Gulf of Maine, indicating that model differences were not due to a significantly different alteration of the shape of the normal mode. We therefore conclude that the different specification of bottom friction in the three-dimensional model did not significantly affect changes to the tide caused by the tidal barrier.

Sensitivity studies with the three-dimensional model showed that retaining convective terms and horizontal eddy viscosity terms for only the vertically averaged mode was a good approximation for the Gulf of Maine. In addition, neglecting the nonlinear terms in the momentum equations that arise from a transformation to a sigma coordinate system is also a good approximation, at least for tidal flows.

6. Future research

Grid scale, particularly in the Bay of Fundy, is an extremely important aspect of tide modeling in the Gulf of Maine. A systematic study on the affect of grid scale on model accuracy is thus warranted. Of course grid scale has traditionally been constrained by computer resources, but as faster computers and more efficient numerical techniques become available this aspect of tide modeling for the Gulf of Maine could be investigated.

The effect of stratification on the eddy viscosity parameter for the three-dimensional model should be included to improve modeled velocity structure, particularly at deeper stations in the Gulf of Maine. The effect of a vertically varying eddy viscosity parameter on calculated velocity profiles should also be examined. The eddy viscosity parameter varies with depth and generally obtains smaller values nearer the surface and bottom than at middepth (Bowden 1959). Tee (1982) found that a vertical eddy viscosity parameter dependent on $z(\sigma)$ was necessary to match tidal velocity profiles in the Bay of Fundy. The incorporation of a vertically varying eddy viscosity into a three-dimensional model of the Gulf of Maine may be necessary to produce a better fit of observed velocity profiles.

Numerically, the incorporation of vertically varying eddy viscosity does not present any difficulties. There are several numerical methods available that incorporate this feature into a tidal model; for example, Pearce and Cooper (1981), Tee (1982), Davies (1986), and Lardner and Cekirge (1988) have all dealt with this problem. The difficulty, however, is that the eddy viscosity is, in general, an unknown tuning parameter. Research to estimate this parameter in various regions of the gulf would thus be warranted. Inverse modeling techniques, such as the method developed by Panchang and O'Brien (1989), may also prove useful in determining the value of the eddy viscosity coefficient from limited velocity data.

Acknowledgments. This research was funded by the University of Maine Sea Grant College Program under grants from NOAA, U.S. Dept. of Commerce, Federal Grant NA-89-AA-D-SG020. This research was conducted using the Cornell National Supercomputer Facility, a resource of the Cornell Theory Center, which receives major funding from the National Science Foundation and IBM Corporation, with additional support from New York State and members of its Corporate Research Institute. We are grateful to David Greenberg for his many insightful comments on this work and to an anonymous reviewer who pointed out several deficiencies in an earlier version.

APPENDIX

Calculated and Observed M_2 Amplitude and Phase at 45 Locations in the Gulf of Maine and Bay of Fundy

The model amplitudes and phases were compared to data for the 45 stations. Stations marked with an asterisk are data taken from Greenberg (1977). All other stations are from Moody (1984). The station names are as found in the original source.

a. 2D and 3D model amplitudes (cm) compared with data

Station number	Name	Amplitude		Percent difference	2D model amplitude	Percent difference
		M_2	2D model			
1	E	0.45	0.44	−2	0.45	−1
2	M7	0.41	0.37	−9	0.39	−5
3	M3	0.40	0.34	−15	0.35	−11
4	M9	0.39	0.38	−1	0.39	0
5	K	0.40	0.37	−7	0.38	−4
6	D	0.77	0.73	−4	0.75	−2
7	M1	0.78	0.76	−3	0.78	0
8	B	0.26	0.21	−19	0.23	−10
9	R	0.31	0.29	−7	0.31	−2
10	S	0.32	0.23	−28	0.30	−8
11	NSFE1	0.39	0.32	−16	0.34	−11
12	Q	0.39	0.35	−9	0.36	−7
13	NSFE2	0.40	0.36	−11	0.37	−9
14	NSFE4	0.42	0.40	−5	0.40	−5
15	P	0.42	0.37	−12	0.37	−11
16	BBA	0.54	0.21	−62	0.24	−56
17	Seal Island	1.20	1.29	7	1.35	12
18	Pinkney	1.55	1.55	0	1.61	4
19	Yarmouth	1.63	1.67	3	1.74	6
20	Port Maitland	1.85	1.83	−1	1.90	2
21	B6	0.88	0.83	−6	0.85	−3
22	Bar Harbor	1.55	1.46	−6	1.50	−3
23	Cashes Ledge	1.20	1.18	−2	1.20	0
24	Rockland	1.50	1.40	−7	1.42	−6
25	Monhegan	1.30	1.27	−2	1.29	−1
26	Nauset	1.03	0.97	−6	0.97	−6
27	Cape Cod	1.16	1.09	−6	1.10	−5
28	Portland	1.33	1.31	−1	1.33	0
29	Cape Porpoise	1.27	1.26	−1	1.28	1
30	Cape Cod Canal	1.24	1.36	9	1.39	12
31	Portsmouth	1.30	1.27	−3	1.29	−1
32	Boston	1.35	1.32	−2	1.34	0
33	Isle Haute	4.19	4.12	−2	4.09	−2
34	Margaretville	3.87	4.02	4	4.01	4
35	St. Martins	3.69	3.72	1	3.68	0
36	Centreville	2.61	2.66	2	2.70	4
37	Dipper Harbor	2.80	2.66	−5	2.66	−5
38	Eastport	2.61	2.54	−3	2.50	−4
39	*Cape Enrage	4.36	4.60	5	4.56	5
40	*Hopewell Cape	4.96	5.02	1	4.98	0
41	*Port Greville	4.61	4.83	5	4.68	2
42	*Dilligent River	4.88	4.98	2	4.82	−1
43	*Five Islands	5.42	5.68	5	5.44	0
44	*Burntcoat Head	5.64	5.91	5	5.68	1
45	*Scots Bay	4.67	4.89	5	4.77	2

b. 2D and 3D model phases (degrees) compared to data

Station number	Name	Phase		Absolute difference	3D phase	Absolute difference
		M_2	2D			
1	E	24	24	0	24	0
2	M7	38	43	−5	44	−6
3	M3	22	24	−2	20	2
4	M9	5	6	−1	4	1
5	K	18	18	0	16	2
6	D	92	98	−6	96	−4
7	M1	92	96	−4	93	−1
8	B	47	70	−23	66	−19
9	R	3	6	−3	1	2
10	S	1	19	−18	23	−22
11	NSFE1	356	360	−4	364	−8
12	Q	353	356	−3	359	−6
13	NSFE2	354	355	−1	358	−4
14	NSFE4	353	352	1	353	0
15	P	352	353	−1	358	−6
16	BBA	8	25	−17	−1	9
17	Seal Island	52	52	0	50	2
18	Pinkney	59	62	−3	60	−1
19	Yarmouth	63	69	−6	67	−4
20	Part Maitland	66	74	−8	72	−6
21	B6	87	89	−2	87	0
22	Bar Harbor	93	93	0	93	0
23	Cashes Ledge	98	99	−1	97	1
24	Rockland	98	99	−1	97	1
25	Monhegan	99	99	0	97	2
26	Nauset	102	115	−13	112	−10
27	Cape Cod	113	112	1	110	3
28	Portland	103	102	1	100	3
29	Cape Porpoise	103	103	0	101	2
30	Cape Cod Canal	109	112	−3	117	−8
31	Portsmouth	107	105	2	103	4
32	Boston	111	108	3	331	0
33	Isle Haute	98	112	−14	114	−16
34	Margaretville	92	108	−16	110	−18
35	St. Martins	102	114	−12	116	−14
36	Centreville	92	98	−6	97	−5
37	Dipper Harbor	98	109	−11	107	−9
38	Eastport	99	105	−6	107	−8
39	*Cape Enrage	104	118	−14	123	−19
40	*Hopewell Cape	109	123	−14	130	−21
41	*Port Greville	109	122	−13	129	−20
42	*Dilligent River	112	124	−12	131	−19
43	*Five Islands	130	134	−4	146	−16
44	*Burntcoat Head	141	135	6	147	−6
45	*Scots Bay	106	119	−13	126	−20

REFERENCES

Bowden, K. F., L. A. Fairbairn, and P. Hughes, 1959: The distribution of shearing stresses in a tidal current. *Geophys. J.*, **2**, 288–304.

Brown, W., 1984: A comparison of Georges Bank, Gulf of Maine and New England shelf tidal dynamics. *J. Phys. Oceanogr.*, **14**, 145–167.

Chu, Wen-sen, J. Liou, and K. D. Flenniken, 1989: Numerical modeling of tide and current in central Puget Sound: A comparison of a three-dimensional and a depth-averaged model. *Water Resour. Res.*, **25**, 721–734.

Cooper, C. K., and B. R. Pearce, 1977: A three-dimensional numerical model to calculate currents in coastal waters utilizing a depth varying vertical eddy viscosity. Rep. No. 226, Ralph M. Parsons Laboratory, Mass. Inst. of Technology, 147 pp.

Csanady, G. T., 1976: Mean circulation in shallow seas. *J. Geophys. Res.*, **81**, 5389–5399.

Davies, A. M., 1986: A three-dimensional model of the northwest European continental shelf, with application to the M_4 tide. *J. Phys. Oceanogr.*, **16**, 797–813.

——, and G. K. Furnes, 1980: Observed and computed M_2 tidal currents in the North Sea. *J. Phys. Oceanogr.*, **10**, 237–257.

Dennis, R. E., and E. E. Long, 1978: A user's guide to a computer program for harmonic analysis of data at tidal frequencies. NOAA Tech. Rep. NOS 41, U.S. Department of Commerce, Rockville, MD, 29 pp.

Duff, G. F. D., 1981: A gulf and ocean model of the Bay of Fundy tides and their response to barrier construction and operation. *Utilitas Mathematica*, **19**, 3–80.

Flather, R. A., 1976: A tide model of the north-west European continental shelf. *Mem. Roy. Soc. Liege*, **10**, 141–164.

Garrett, C., 1974: Normal modes of the Bay of Fundy and Gulf of Maine. *Can. J. Earth Sci.*, **11**, 549–556.

——, J. R. Keeley, and D. A. Greenberg, 1978: Tidal mixing versus thermal stratification in the Bay of Fundy and Gulf of Maine. *Atmos.-Ocean*, **16**, 403–423.

Gill, A. E., 1982: *Atmosphere-Ocean Dynamics*, Academic Press, 662 pp.

Greenberg, D. A., 1977: Mathematical studies of tidal behaviour in the Bay of Fundy. Manuscript Report No. 46, Dept. of Fish., Ottawa, Canada.

——, 1979: A numerical model investigation of tidal phenomena in the Bay of Fundy and Gulf of Maine. *Mar. Geod.*, **2**, 161–187.

——, 1983: Modeling the mean barotropic circulation in the Bay of Fundy and Gulf of Maine. *J. Phys. Oceanogr.*, **13**, 886–904.

Lardner, R. W., and H. M. Cekirge, 1988: A new algorithm for three-dimensional tidal and storm surge computations. *Appl. Math. Modeling*, **12**, 471–481.

Loder, J. W., and D. G. Wright, 1985: Tidal rectification and frontal circulation on the sides of Georges Bank. *J. Mar. Res.*, **43**, 581–604.

Moody, J. A., B. Butman, R. C. Beardsley, and coauthors, 1984: Atlas of tidal elevation and current observations on the northeast American continental shelf and slope. *USGS Survey Bull. 1611*, Alexandria, VA 22304. 112 pp.

Nihoul, J. C. J., 1982: *Hydrodynamic Models of Shallow Continental Seas*, Elsevier, 41–67.

Panchang, V. G., and J. J. O'Brien, 1989: On the determination of hydraulic model parameters using the strong constraint formulation. *Modelling Marine Systems, Vol. 1*, 5–18.

Pearce, B. R., and C. K. Cooper, 1981: Numerical circulation model for wind induced flow. *J. Hydraulics Division*, ASCE, **107**, 285–302.

——, ——, and E. Doyle, 1979: Hurricane generated currents. *Proc. ASCE Specialty Conf. on Civil Engineering in the Oceans IV*. San Francisco, CA, 398–415.

Prandle, D., 1982: The vertical structure of tidal currents and other oscillatory flows. *Contin. Shelf Res.*, **1**, 191–207.

Schwiderski, E. W., 1980: Ocean tides. Part II: A hydrodynamic interpolation model. *Mar. Geod.*, **3**, 219–255.

Sucsy, P., 1990: Two- and three-dimensional tide model studies in the Gulf of Maine. Ph.D dissertation. Dept. of Civil Engineering, University of Maine, Orono, ME 04469. 233 pp.

——, B. R. Pearce, and V. G. Panchang, 1990: Sensitivity of Gulf of Maine tide model to depth. *Estuarine and Coastal Modelling*, Malcolm L. Spaulding, ASCE. 268–277.

Tee, K. T., 1982: The structure of three-dimensional tide-generating currents: Experimental verification of a theoretical model. *Estuar., Coastal Shelf Sci.*, **14**, 27–48.

Townsend, D. W., J. P. Christensen, D. K. Stevenson, and coauthors, 1987: The importance of a plume of tidally-mixed water to the biological oceanography of the Gulf of Maine. *J. Mar. Res.*, **45**, 699–728.

Wright, D. G., and J. W. Loder, 1985: A depth-dependent study of the topographic rectification of tidal currents. *Geophys. Astrophys. Fluid Dyn.*, **31**, 169–220.

Yentsch, C. S., and N. Garfield, III, 1981: Principal areas of vertical mixing in the waters of the Gulf of Maine, with reference to the total productivity in the area. *Oceanography from Space*, J. F. R. Gower, Ed., Plenum Press, 303–312.